Chapter 10

Patterned Nanomagnetic Films

J. Cock Lodder
Systems & Materials for Information storage,
MESA+ Institute for Nanotechnology, University of Twente, POBox 217,
7500AE Enschede The Netherlands.

Abstract Nano-fabrication technologies for patterned structures made from thin films are reviewed. A classification is made to divide the patterning technologies in two groups namely with and without the using a mask. The more traditional methods as well as a few new methods are discussed al in relation with the application. As mask less methods we discussed direct patterning with ions including FIB, nanopaterning with electron beams, interferometric laser annealing and ion beam induced chemical vapor deposition. The methods using masks are ion irradiation and projection, interference lithography, the use of pre-etched substrates and templates from diblock copolymers and imprint technologies. Also a few remarks are given concerning the magnetic properties of patterned films. Nanometer scale magnetic entities (nanoelements, nanodots, nanomagnets) form a fast growing new area of solid-state physics including the new fields of applications. Two of them are summarized namely media for ultra high-density recording and magnetic logic devices.

1. INTRODUCTION

Patterned magnetic nanostructures are researched and developed for fundamental studies and applications in areas such as nanomagnets, ultra high-density storage, spinelectronic devices, memory cells (MRAM) magnetic logic. Recently a few overview papers about nanostructuring and related properties have been published [1-3]. Many methods are used to make small magnetic structures from sub micron scale down to nanometer dimensions. They have been made either in single dots or periodic structures such as arrays in rectangular or hexagonal shape depending of the type of study and application. In the literature the fabrication of magnetic nanostructures have been reported either by using the top-down as well as the bottom–up strategy. In this chapter we will focus on the methods following the top down approach. This type of patterned structures can be made by one process step technique (deposition through a shadow mask) or

via a multi-process step such as using photoresist, etching, lift-off techniques etc. Patterns with nano-dimensions cannot be prepared by standard-optical lithography and therefore other methods are used such as: electron-beam lithography, X-ray lithography, nanoimprint lithography, and interference lithography. But also Focused Ion Beam techniques, nano-imprint and diblock copolymer template technologies are use for realizing nanostructures in magnetic thin films.

It is well known that the magnetic properties from a ferromagnetic bulk material differ with the same material in thin film form. In addition a comparison between a patterned structures will show different magnetic properties from their parent thin film material. In general a magnetic material can change its magnetization either by domain wall motion or by one of the rotation mechanisms. Figure 1 illustrates how the domain structure and in connection the reversal mechanism changes as function of the size. In this case the continuous Co/Pt multilayer film, with a perpendicular anisotropy, shows a typical stripe domain structure. The patterned structures are made by interference lithography (IL) and dry etching After patterning the dots of 180 nm are still multi-domain (MD) but if they have a size of 70 nm only the single domain (SD) state with was detected in the MFM observations.

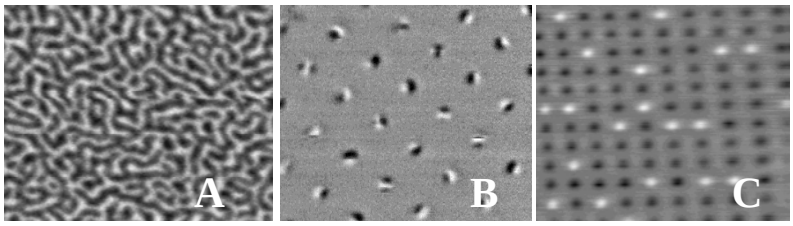

Figure 1. MFM image (4mm x 4mm) from a Co/Pt multilayer continuous film (A), arrays of MD dots of 180 nm (B) and SD dots of 70 nm (C)).

Another example showing the influence of the shape on the magnetic behavior of a nanostructure is discussed in [4]. Here experiments and theory have been carried out on various shaped dots of Supermalloy (Ni-Fe-Mo alloy) made by e-beam lithography. They show, as prepared, an in-plane isotropic anisotropy The various shapes of the magnetic dots (squares, triangle or pentagon) have a great impact on the magnetic anisotropy and related properties. This type of films show in addition the phenomenon of configurational anisotropy. Configurational anisotropy is related to the role

played by small deviations from uniformity in the magnetization field within the nanostructures, which allow unexpected higher-order anisotropy terms to appear. But also the competition that exists between exchange energy and magnetostatic energy plays an important role. This competition determines whether the nanostructures exhibit single domain or incoherent magnetization and also controls the non-uniformities in magnetization, which lead to configurational anisotropy [4].

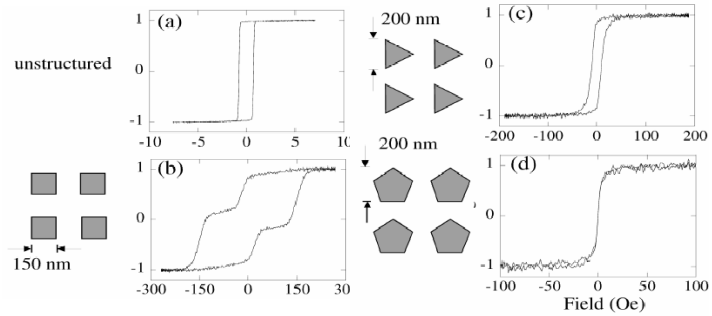

Figure 2. Hystheresis loops as a function of the various shapes squares (b), triangles (c) and pentagons (d) of patterned structures of Supermalloy and the continuous film (a).

Hysteresis loops measured form a continuous film and various shapes of nanostructures from Supermalloy are given in Fig.2. The thickness of the various films are 6nm (a), 5nm (b), 5nm (c) and 3 nm (d). The applied field is assumed to point up the page. Understanding the influence of shape opens the way to designing new nanostructured magnetic materials where the magnetic properties can be tailored to a particular application with a very high degree of precision. It has been determine by that the triangle shape exhibit a 6-fold, square shape a 4-fold and the pentagonal structures a 10-fold anisotropy. [4,5].

2. PATTERNING TECHNOLOGIES FOR MAGNETIC THIN FILMS

It is generally realized that for sub-100 nm structures a new generation of lithography techniques needs to be developed. For the preparation of limited numbers of nanosized structures, electron beam lithography (EBL) is more or less the standard patterning technology. But direct e-beam writing is a very slow process in the case large areas sould be covered.

Using EBL or ion beam lithography (IBL) a variation of shapes and dimensions can bee realized even down to 10 nm in size. With EBL large areas cannot be made accurately due to the problems with the long-range coherence of the e-beam writer and also the throughput is very low. But it is a very flexible method for the fabrication of nanostructures of arbitrary shapes for research [e.g.4]. Recently it has been shown that EB and IB projection methods can solve the problems with the throughput and mis-coherence [6]. Other lithography methods such as X-ray lithography and nanoimprint lithography (contact lithography) and the mask less interference lithography are also used for making large areas of nanostructures. Soft X-rays (λ = 0.5 – 4.0 nm) lithography is using a thin (about 2 micron) mask just above the sample with the resist layer. The mask is mostly prepared form silicon carbide covered by a metallic pattern (with high absorbing materials such as gold, tantalum or tungsten) with the designed geometry. The advantage is that the mask can be used repeatedly.

Nanoimprint lithography is a fast growing technology and is principally different from the conventional lithographical methods. It has two steps namely imprint and pattern transfer and was proposed in 1995 [8]. The mold with the nanostructures at the surface is pressed into a resist layer on the substrate. The imprint can be carried out by a temperature of about 120C at a pressure of 30- 50 bars. The parameters are of course depending on the type of resist used. Sub-10 nm features and 40 nm pitch on Si as well as on Au substrates has been demonstrated [8]. The mask and the master mold used by the two lithographic techniques mentioned above have to be manufactured by using other lithography methods such as e-beam, nanoimprint or interference lithography (IL). In the case of IL a resist layer is exposed by an interference pattern generated by two obliquely incident beams (laser or X-rays). With one exposure resist lines are produced having a period of half the wavelength used. After rotating the sample over 90 degrees a second exposure can be given and after that this illumination dot arrays can be produced.

It is arbitrary to make a classification about the avaiable technologies for making nanostructured magnetic films. In this paper we follow two routes namely direct writing and writing by the use of a mask. Direct writing can be carried out by using ion beam, e-beam and laser interference annealing. If a mask is used methods as ion irradiation, interference lithography, imprint technology and block copolymer templates can be mentioned.

2.1. Mask less thin film patterning

Instead of using resist layers for pattern definition, the desired pattern may also be directly written in the magnetic layer or even be directly deposited. Mask less nanopatterning includes ion and electron beam direct irradiation of the film and also a method called laser interference annealing. Irradiation and annealing the film can influence anisotropy or magnetization by changing the phase and or chemical composition of the film locally or over a large area. Also other methods are discussed such as, laser-assisted direct imprint, ion-beam-induced chemical vapor deposition (IBICVD), and ion projection patterning.

2.1.1. Direct pattering with ions

The use of energetic ion irradiation to alter the properties of magnetic films and multilayers has attracted increasing interest in recent years. When ions interact with the surface, many effects occur, such as radiation damage, elastic reflected ions, implantation and ion etching (milling). The magnetic properties such as coercive field [9-11] anisotropy field [12] and exchange biasing [13] can be locally and controllably changed to engineer the behavior of small magnetic devices. Especially multilayer structures are very sensitive for ion irradiation due to the sensitive area of the interface between the ferromagnet and metal layers. A good example is the research carried out on Co/Pt films with perpendicular anisotropy. The multilayers are studied before and after ion irradiation and a model about the mechanism of the destroying interface is given in [12]. The Co atoms moving in the ion direction travel more than one interatomic distance and become an isolated (Co-Pt alloy), whereas Co atom moving in opposite direction travel typically only one interatomic distance and contribute to the roughness (local thickness fluctuations). The 'rough' interface will change the magnetic properties a lot. With this technology one can locally change the magnetic state of a sample. Irradiation studies on magnetic multilayers are first published by Traverse et al. [14] studying, e.g. Ni/Au multilayers using fluencies between $2\ 10^{14}$ and $2\ 10^{16}$ ion/cm^2 of 30 keV He^+ ions.
Patterned media (e.g. section 4.1) can be fabricated from magnetic multilayers where ion irradiation is used to differentiate nanoscale magnetic islands in a magnetic matrix, without the removal of material from the multilayers [15,16]. Arrays of Pt/Co/Pt dots with a dot separation of only 20 nm have been showed by FIB irradiation of 28keV Ga+ ions [17]. The

magnetic effects can be influenced by the kinds of ions (He+, Ar+, Ga+, N+), their energies as well as their exposure doses (fluency).

2.1.1.1 Milling with Focused Ion Beam (FIB)

Patterned structures from films can also be made by removing material by ion-milling/etching. Mostly an Focused Ion Beam (FIB) is used as instrument. Besides, Co/Pt multilayers, perpendicular granular CoCrPt films (20 nm thick) have been prepared using FIB [18]. The patterns are directly made in the film by using 30 keV Ga+ at a beam current of 1 pA. MFM and AFM images of the directly patterned film are given in Fig.3.

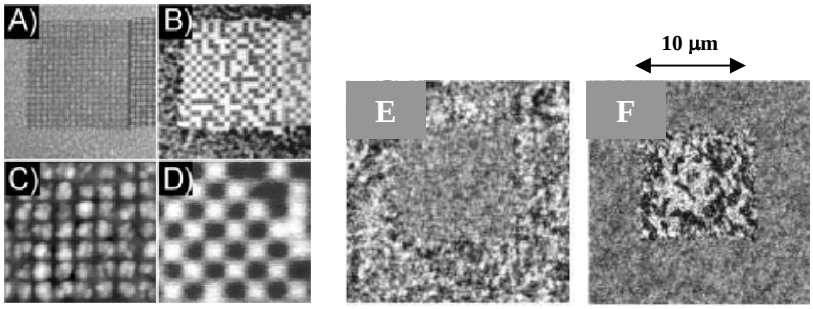

Figure 3. AFM (A and C) and MFM images (B and D) of a CoCrPt thin film medium directly patterned by FIB. Magnetic-domain images taken by spin-SEM after electron bombardment of a centered square for 1200 s; (E) in-plane, and (F) out-of-plane magnetization component.

The pattern trenches are 6 nm deep and square arrays of magnetic isolated islands have been prepared in the range 65-500 nm. Figure 3(A) shows an array of 2x2 mm^2 patterned into a period of 20 x 20 islands with100 nm period and 70 nm side-length. The MFM images (B&D) are made after AC demagnetization procedure of the sample using a perpendicular field from 20 to 100 Oe. With a quasi-static write/read tester, recording experiments have been performed (see section 4.1).

2.1.1. Direct nanopaterning with e-beam

Intense electron beams with keV energy can modify magnetic anisotropies locally. In [19] it has been shown that in very thin epitaxial Co films the easy axis switch from parallel to perpendicular to the surface while the domain size can be enlarged by one order of magnitude. In this paper it has been

shown that local magnetic modifications can bee 'written' without adding or removing atoms or molecules The e-beam of a SEM was used to scan the surface with an operating voltage of 10 keV. A maximum beam current at the sample position of 10 nA was achieved by removing the objective aperture of the microscope. Total exposure times were varied from 10 to 1200 s. The principle of local magnetic modification is illustrated in Fig.3(E&F). The electron beam scanned an area from 18x18 mm^2. The irradiation in the square corresponds to a dose of 2.4 x 10^{10} electrons/mm^2. The spin-SEM image is taken form both the electron-beam-treated area and its surroundings. Within the square, the magnetization direction has switched completely from in-plane to out-of-plane as shown by the uniform gray level in Fig.3(E) and the black/white contrast in Fig.3(F).

Another application of direct e-beam irradiation is given in [20]. In this paper, non-ferromagnetic Co-C thin films were magnetically patterned using a focused electron beam with a probe diameter of less than 0.1 m. The as deposited film shows a superparamagnetic behavior but after an anneal process (400-500 C) the film becomes ferromagnetic. The smallest magnetic dot diameter is about 270 nm. By the use of AFM and MFM characterization the physical dot size and the magnetic dots size can be determined.

In Fig.4A it can be seen that he AFM dot size is almost independent on the dwell time (e-beam irradiation time) while the magnetic dot diameter (MFM) increases almost linearly with the square rote of the dwell time.

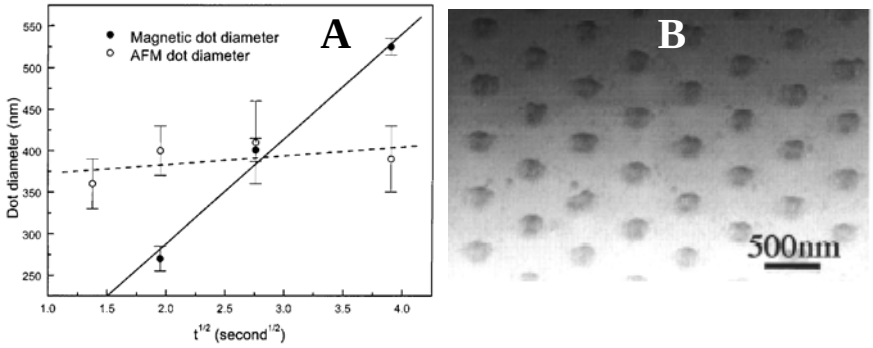

Figure 4. (A) Time dependence of AFM (open circle) and magnetic (solid circle) dot size and (B) TEM micrograph of a patterned Co-C film with direct laser lithography

The dependence of 'square root of dwell time per dot', means that the magnetic dots are produced by heat-conduction- induced phase change in the film.

2.1.3. Interferometric Laser Annealing

Laser interference can be used as a lithography method and is particularly suitable for realizing periodic structures in resists The resist is exposed to a standing wave pattern generated by the interference of two laser beams (see also section 2.2.3.) This interference will give a line pattern with a periodicity (Λgiven by λ/ 2sinθ), where λ is the wavelength and θ the angle between the incidence light and the sample normal. By changing θ the periodicity can easily be adjusted from 700 nm down to 100 nm. Hexagonal or cubic patterns are made by double exposure with the sample rotated 60 or 90 degrees between the exposures. Direct laser interference annealing is applied directly on a magnetic thin film. It produces a 2-dimensional hexagonal dot array. This method has been explained in [21] and applied to sputtered non-magnetic Co-C thin films of 40 nm thick. An excimer laser having a wavelength of 308 nm was used and exposed to a 10-ns-pulsed and a flux of 0.17 J/cm2. The laser beam was split into two beams generating an interference pattern and a periodic modulation of the light intensity. The size and shape of the regions depend on the incident angles of the beam, on the pulse duration, and on the flux. The as-deposited Co-C films are more or less amorphous and in this state the films are not ferromagnetic at RT. After annealing (350-550C) the magnetic Co nanoparticles are formed with diameters of 1—25 nm. The use of Co-C films was chosen because they form a simple system containing immiscible Co carbides decompose easily into Co and C upon annealing [22]. Figure 4B shows a TEM image of a Co-C film after laser annealing. The dots are 250 nm in diameter and the dot spacing is 650 nm. Dots as well as the matrix are showing a granular structure with 1-2 nm grains with evidence for slightly more order in the dot area [21].

2.1.4. Ion beam induced Chemical Vapor Deposition

This method can be compared with Ion Beam Assisted Deposition (IBAD) where the arriving atoms on the substrate receive an additional energy for the growth by ions. In the case of ion beam induced CVD there is a momentum and energy exchange between incident ion beam (Ga^+) and the molecules of a precursor. Besides the ‘milling’ capacities of the FIB this machine can be used also for deposition of materials in almost arbitrary shape. The principle of FIB deposition is localized chemical vapor

deposition (CVD) by a direct writing technique. The reactions occurring during deposition of metals and insulators are well comparable to, for example, laser-induced CVD [e.g.28]. Patterns of deposited areas are fabricated through vector scan rastering. For our application the precursor is suitable for creating a ferromagnetic metal. In the case of Co deposition di-cobalt octacarbonyl has been used. The method is up to now only described for FeCo, CoPt etc materials which can be eventually be applied as a magnetic dot array medium for future data storage applications.

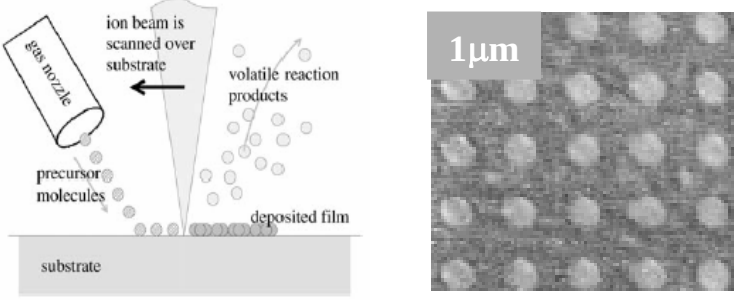

Figure 5. (Left).The principle of ion–induced deposition and (Right) FIB in-situ imaging of Co dots (800nm diameter) fabricated by IBICVD technology

The deposition process is illustrated in Fig.5(left). The precursor gases are sprayed on the surface by the 'nozzle', where they are adsorbed. In a second step, the incoming ion beam decomposes the adsorbed precursor gases. Then the volatile reaction products desorb from the surface and are removed through the vacuum system, while the desired reaction products remain fixed on the surface as a thin film. The deposited material is not fully pure however, because organic contaminants as well as Ga ions (from the ion beam) are inevitably included in the deposited film [23].
Figure 5(right) shows an array of 800nm Co dots, spaced form each other by 800nm. Also smaller dot size (150nm) has been prepared. The improvement is achieved mostly due the selection of a proper substrate that minimizes surface diffusion and mixing within the surface region. Further optimizations may lead to dot sizes with a factor 2-5 smaller [24].

2.2 Patterning with masks

The most principle idea about a patterning process for a thin film is that the film on the substrate is covered with a spinned layer of resist and the pattern

is exposed in the resist through a mask. Finally the resist layer or other layers can be used as ‘masks’ during the following process-step. From the IC-technology it is known that many ‘mask’ are necessary to final the device. The 2D pattern is transformed into a 3D resist structure and further after processing in the thin film. Developing the resist various profiles are made depending on the developer, the type of resist, the developing time and temperature. Patterning transfer is than realized by etching the thin film. This can be done by wet-chemical as well as by dry-etching methods. Finally a solvent or a dry etching method will strip the remaining resist. An alternative to realize structures is using the lift-off technique. In this case the resist structure is formed on the substrate and the film is deposited through the openings/holes and on the resist surface. While the resist is stripped the material deposit on the resist is lifted off while the film on the substrate remains. Frequently one can find electrodeposition in combination with post-lithographical processes. In this case the substrate should be conductive or should first be coated with a conductive layer.

2.2.1. Ion irradiation through a mask

Here the magnetic properties are modified by irradiation (see also section 2.1.1.) of the material through a lithographically defined mask. Good examples of the effect of irradiation is given by [25] where ion irradiation is used to alter the direction and angular dispersion of the anisotropy in sputtered soft magnetic NiFe films of 5 nm thickness. During the irradiation in some cases an applied field of 400–700 Oe in a specified direction at the samples was present. The fluency was between 10^{13} and 10^{16} ion/cm^2 while 200 keV Ar^+ ions where used. Anisotropy direction and angular dispersion were determined by angle-dependent remanence measurements [26]. From this the conclusion can taken that ion irradiation can be used to either increase or decrease dispersion in this film. In Fig.6(left) the effect of ion irradiation through a mask is shown for a Permalloy thin film. The energy deposited by the ions allows for the movement of the sample atoms, most likely through a series of direct collisions. Much as an applied field during film growth or thermal annealing can be used to affect the bulk magnetic anisotropy of a sample, an applied field during irradiation encourages magnetic ordering along the field direction where ions traverse the film. Thus a film can be anisotropy patterned by irradiation through a mask with the annealing field set along any direction. The minimum feature size attainable by this technique will most probably be set by the feature size of

the mask (or extent of a focused ion beam), and therefore should be on the order of 10 nm [25].

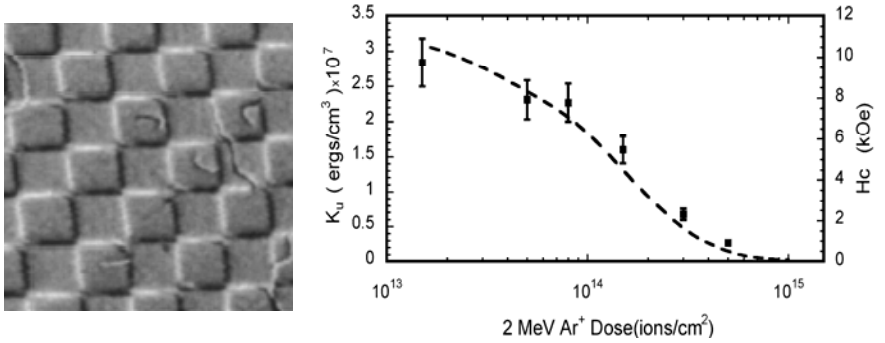

Figure 6. (Left) MFM micrograph of a NiFe film with 10 mm square magnetic domains and (Right) Perpendicular anisotropy (Ku) and Hc on exposure to 2 MeV Ar+ for Co/Pt samples

Many papers by have been published about studying this irradiation mechanism for modifying Co/Pt like multilayers having a perpendicular anisotropy (see also section 2.1.1). In [27] fluencies between 2x 10^{14} - 2x 10^{16} ions/cm^2 have been used at 30 keV He^+ ions. The He^+ ions do not etch the sample and initial roughness is preserved, but the result is a decrease of magnetic anisotropy, coercivity and Curie temperature. Consequently, in Co/Pt multilayers can change the anisotropy form perpendicular in the in-plane direction or even the unprotected areas can be changed into the paramagnetic state. The mechanism behind this is still in discussion not very well understood and in [9,12] local atomic relaxation (see also section 2.1.1.) and alloy formation is given while in the authors in [28], using 700 keV N^+ ions, found direct evidence for local atomic displacements at the Co/Pt interface which destroys the anisotropy. The dose required initiating spin reorientation scales with the interface anisotropy Ks of the films used in [28]. For a film with high Ks ~ 85 erg/cm^2 they need 1.5 10^{15} N^+ /cm^2 while for a film Ks ~ 4 erg/cm^2 6 10^{14} N^+ /cm^2 is necessary. It is roughly equal to the numbers of Co interface atoms per unit interface area contributing to Ks [28]. Irradiation studies of Co/Pt with different energies and ion species (20 keV He^+, 2 MeV H^+, 20 keV Ar^+, 2 MeV Ar^+, 30 keV Ga^+) using doses (10^{11}-10^{17} ions/cm^2) have been carried out [29] .For the same amount of intermixing the dose of He+ can be replaced by heavier ions such as Ar^+ (100 fold) of the same energy and 400-fold for Xe^+.

In Fig.6(right) the perpendicular anisotropy Ku (=Kv+ 2 Ks/t) are given as a function of the exposure of 2 MeV Ar^+ for a Co/Pt multilayer. In this case the Ku is determined by a contribution from the volume anisotropy (Kv) and the interface anisotropy (Ks) and the thickness of the ferromagnetic layer (t). The conclusion is that the fall of the coercivity with dose reflects a reduction in the perpendicular anisotropy associated with intermixing of the Co/Pt interfaces [29]. In this paper it is conclude that the multilayers are very sensitive to irradiation than expected on the basis of nearest-neighbor coupling and simple ion-beam mixing. It is also stated that the ion irradiation effect strongly depends on the type of samples one made. Moreover the mask lifetime is also a concern as well as the surface roughness of the irradiated areas. Also for this the fluency and energy as well as the use of seedlayers and substrate must be optimized. Comparison of the dependence of perpendicular anisotropy Ku and coercivity Hc on exposure to 2 MeV Ar+ for Co/Pt multilayer samples. The data points show the anisotropies as determined with VSM (left scale). The Ms values used to calculate the 2 μMs^2 term were; 450 emu/cm^3, except for the point at $5x10^{14}$ ions/cm^2, where it had fallen to about 250 emu/cm^3. The dashed line follows coercivities obtained for Kerr rotations for the same samples (see right scale of Fig. 6(right)). Anisotropy also can be engineered to be out-of-plane and in-plane alternatively by using selective epitaxial growth. In [30] an approach to anisotropic patterning for Ni films is reported by using selective epitaxial growth. In this method, a modulated single/polycrystalline substrate surface was used to modify locally the magnetic anisotropy in subsequently deposited magnetic films, which induces the desired artificial magnetic structure. Consequently the Ni film has a spatially varying anisotropy via selective epitaxial growth.

2.2.2. Ion projection direct structuring (IPDS)

In the previous section we have seen that irradiation with ions can (locally) modify the magnetic properties of the materials such as Co/Pt multilayers. Direct writing with ion, like e-beam writing, is a slow process. IPDS [6] facilitates a large-area pattering process. It is a non-contact process, which preserve the as-grown surface structures. The mask (mostly SiO_2) consists of all structures necessary for hard disk drives such as bit cells in a circle arrangement and servo (head positioning) structures. PPDS transfer the mask structure with a demagnification factor 4 into the magnetic medium. The exposure was carried out with He+ ions having a dose of 2 10^{15} He^+ /cm^2 at

45 keV in Co/Pt multilayer. The ion energy at the mask is lower than the ion energy at the Co/Pt layer, and moreover the medium is at a significant distance from the masks. This method is proposed for commercialization to fabricate the future hard disks media.

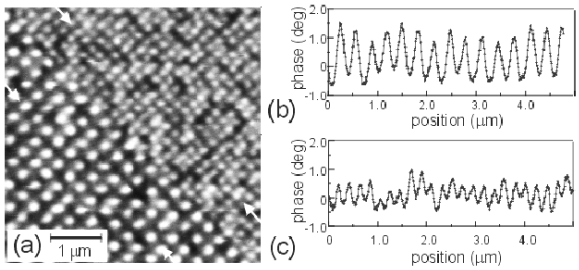

Figure 7. MFM image (a) and analyses (band c) of irradiated Co/Pt multilayer through a stencil mask. Lines scans from lower left and upper right part along rows of dots as indicated by white arrows are given in b) and c) respectively.

Circular tracks of 17 mm in diameter containing data and servo structures were structured [6]. The proposed IPDS technology shows a direct structuring process without any contact with the surface of the structured surface is also described in [31]. In Fig.7 the MFM analysis is given for a Co/Pt multilayer irradiated through a stencil mask with Cartesian dot configuration showing 86 nm dots at a 344 nm pitch in the lower left part and 57 nm dots at 230 nm pitch in the upper right part. The lines scans from the lower left and the upper right along rows of dots as indicated by white arrows are given in b) and c) respectively (see also [6]). The authors are planning to improve their machine and stated that a storage capacity of 1 Tb/in^2 could realistically obtained.

2.2.3. Interference lithography

With interference lithography (IL) a resist layer is exposed by an interference pattern generated by two obliquely incident laser beams, which is used to expose a photoresist layer without the use of a mask.(see section 2.1.3.). Dots can simply be fabricated by a second exposure after rotating the substrate over 90°. The patterned area is determined by the diameter of the two laser beams. For processes with no need for alignment, IL is relatively simple and cheap. The method is already used for more than 20 years for the preparation of submicron gratings for application in integrated optics [32]. In

recent years, the possibility of patterning large areas of dots with IL has been recognized. Now, IL is attracting great attention for a wide variety of applications, amongst others: field emission displays, antireflection-structures, photonic crystals, micro filtration and mask making for nanoimprint [41] and X-ray lithography [35] and patterned magnetic media [35-37]. Its capability for patterning large areas is clearly demonstrated by the fabrication of 50 x 50 cm^2 areas of submicron dots [38].

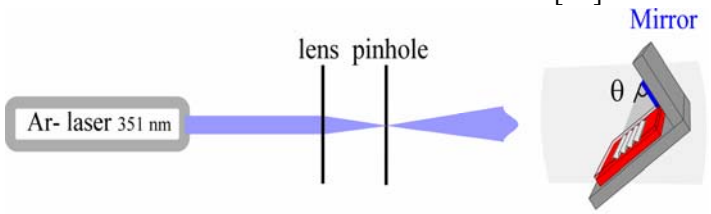

Figure 8. LIL set up for making 2D patterns in a photoresist on top of a thin magnetic film.

Two IL methods have been used for preparing magnetic dots, namely the simple Lloyd's mirror (Fig. 8) consist of a mirror mounted perpendicular to the substrate [37] and achromatic interference lithography (AIL) [39]. For the preparation of isolated magnetic dots by IL, several processing schemes have been developed and are based on the deposition in resist holes by electroplating [36] or evaporation-and-lift-off [35], or on the selective removal of sputter-deposited material by etching [37]. Figure 9a shows IL resist pattern on top of the Co/Pt multilayer (30 nm thick) using a 351-nm laser. A TEM cross-section is shown in Fig.9b, after etching the resist and the Co/Pt. The etching has been stopped in the SiO_2/Si substrate. The obtained dots looks like SD with a diameter of 70 nm dots with a period of 200 nm (see Fig.1C). IL was also shown with a laser wavelength of 257 nm and application of deep UV-resists with high contrast [40]. Lasers with even smaller wavelength have poor temporal and spatial coherence, and are therefore not suitable for laser IL. However, achromatic interference lithography with ArF excimer lasers at 193 nm has the capability of patterning resist structures with periods of 100-nm [41]. The principle of the technique is the use of an exposure set-up with vanishing small difference in the length of the two light paths. It also has been shown that the proposed technique could be expanded for the patterning of structures with 50-nm period [41]. In order to produce the smallest possible interference patterns, there should be a compromise between wavelength and stability of the laser source. Pulsed lasers have a short wavelength, but suffer from a poor

coherency length. For our LIL setup we chose a highly stable continuous wave (CW) YAG laser with a basic wavelength of 1064 nm.

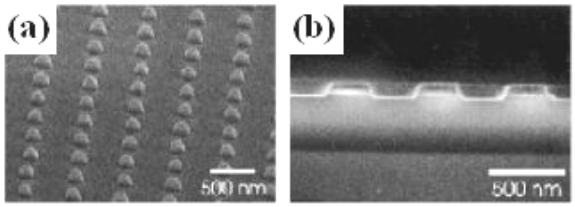

Figure 9. Patterns made by IL using Co/Pt multilayers cover with resist top of the Co/Pt layer (a), TEM cross section of the ion etched structure through the Co/Pt in the Si substrate (b).

This wavelength is frequency-doubled to 532 nm in an intra-cavity. By using an external frequency doubler this wavelength is again halved to λ=266nm with a small bandwidth (1 MHz). This UV laser beam is optically filtered with an 11 mm lens and a 5 mm pinhole to achieve a clean near-Gaussian beam. This diverging beam travels 2.25 m over an optical table to a Lloyd's Mirror Interferometer mounted on a rotation table. The UV beam illuminates both the mirror and the sample. Part of the light reflects on the mirror and interferes with the portion of the beam that is directly illuminating the sample. To prevent vibrations, which could disturb the interference pattern, the whole setup is built on an actively damped optical table of 3x3.6 m. The Lloyd's Mirror Interferometer is placed in a closed cabinet to avoid air movements, which could affect the stability of the interference pattern. With this setup highly regular patterns can be produced over areas of about 2x2 cm^2 [42].

2.2.4. Using pre-etched substrates

Depositing the magnetic material on a patterned Si wafer can also make patterned media. Patterning can be carried out by e-beam lithography followed by RIE and by nano-imprint technologies (see Section 2.2.5). In Fig.10 the principle of the deposition of a pre-etched Si wafer is given. The TEM cross section shows the covering with the deposited multilayer of Co/Pt. In this case the Co is deposited normal to the surface and the Pt at oblique incidence from the right. Consequently, the sidewall B consists of Pt grains with a thickness close to the nominal. The sidewall A is covered with a very thin layer of Co-oxide [43]. In the groove opposite to the Pt-source

the Si can see a discontinuity on place-C due to the shadowing of Pt. It can be concluded that both sidewalls are non-magnetic, consequently no direct exchange between the top and the bottom of the grooves [43]. Areas of dots with pitch of 60 nm were prepared by using nanoimprint technology.

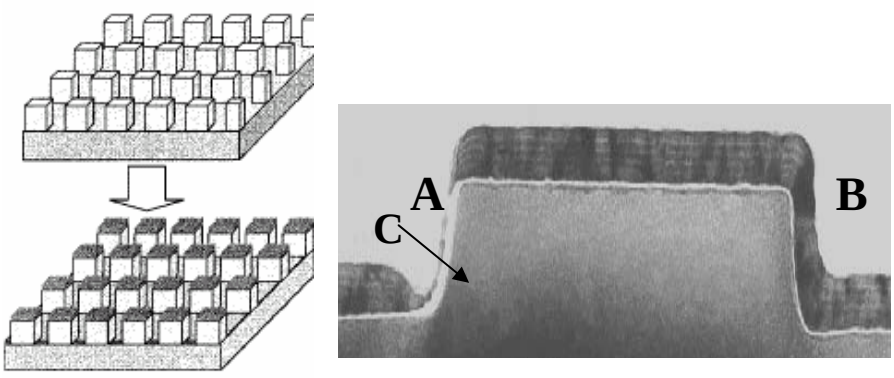

Figure 10. The principle of using pre-etched Si substrates (left top) deposited with a multilayer (bottom left). The TEM cross-section image (right) shows how the multilayer covers the Si structure.

Co/Pt dots do have very high coercivity, which is much larger than the maximum magnetostatic field; consequently the dots are very stable. Write and readback are investigated and it has been demonstrated that it is possible to address individual dots in these arrays, both in the down-track and cross-track directions.

2.2.5. Imprint technology

Contact lithography can offer a high resolution and is in principle less expensive than the optical lithographic methods. It uses a method similar as in optical disk fabrication. It has been demonstrated that imprint technology using compression molding of thermoplastic polymers can produce vias and trenches with 25-nm minimum feature size and 100-nm depth in thin polymer [7]. Nanoimprint is using a mold (master) for deforming the resist. This master can be made either by Interference lithography, E-beam lithography or X-ray lithography. Before starting the imprint a polymer is spin coated on the substrate (covered or not with a thin film). This monolayer is about 30 nm thick.. After heating, by hot emboss technology or

UV-irradiation, one type of the polymer becomes hard and the other soft for reactive ion etching. It is also possible to use the technology without heating but than by using a very high pressure at room temperature [44]. An important aspect in this technology is of course the reliability and accuracy of the imprint stamp (master). A uniform imprint of 100 nm wide lines has been realized on a 6-in Si wafer [45]. Another technology of mold lithography using a photo-curing polymer has proved that sub-100 nm structures can be realized [46]; an automated tool for step and flash imprint lithography has been constructed for using 200 mm wafers [47]. Sub-10 nm structures have been shown from metal dots with a period of 40 nm and a diameter of 10 nm. This tool allows an operator to run automated imprinting experiments without human intervention, except for installation of templates, and loading and unloading of wafers. Imprint templates were treated with a low surface energy self-assembled monolayer to aid selective release at the template-etch barrier interface [47].

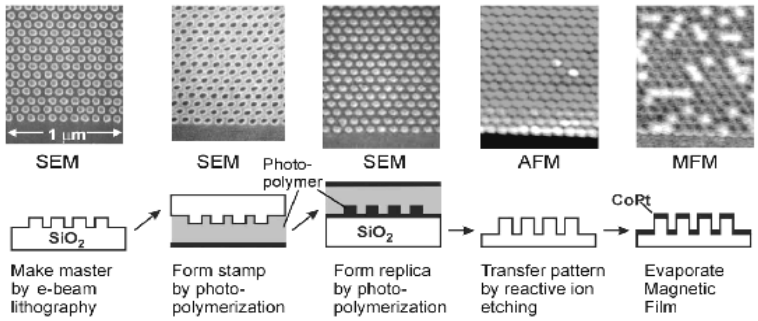

Figure 11. Total process van imprint technology started with mastering, first stamp, replacing the stamp into a flexible stamp, transferring the pattern and finally depositing the Co/Pt multilayer.

These imprint technologies can be combined with various techniques such as electroplating into holes as demonstrated in [33], showing the quantised magnetic disk having perpendicular anisotropy by Ni pillars (diameter=110 nm) in a non-magnetic matrix. Large area magnetic patterning is also described. In [48] a nanomolding process for producing 55-nm-diameter magnetic islands over 3-cm-wide areas is described. The fabrication steps are given in Fig.12 consisting of mastering by EBL, stamping, replication, patterned transferring and deposition of the magnetic layer. Finally, an 11-nm-CoPt multilayer is deposited onto a substrate consisting of a pattern of

pillars 28 nm high. Magnetic force microscopy reveals that the film on top of each pillar is a magnetically isolated single domain that switches independently (see Fig.11). With this process [48], a nearly unlimited number of stamps can be made from a single master, because no hard surface comes in contact with the master during stamp formation, and any residue can be removed nondestructively. In addition to accommodating substrate curvature and roughness, the use of a flexible stamp gives a process less sensitive to localized contamination. If this process can be optimized to form a large number of replicas from each stamp, it may be suitable for large-scale manufacturing.

The combination EBL and imprint technology has been optimized by using PMMA (Poly Methyl MethAcrylate) resist, lift-off technique and reactive ion etching (REI) [49]. The authors where able to fabricate dot arrays pitches and periods down to 30 and 40 nm, respectively. Their SiO_2 pillars can be used to fabricate robust molds for imprint lithography up to densities of 700 Gbpsi. These molds have been tested for imprinting experiments, and good replication was achieved for arrays down to a pitch of 50 nm.

Imprint lithography also have several limitations for many applications because it can in principle only be used for small periodic structures. A general fabrication technology for all kinds of applications should be able to realize various combinations and distributions of large as well as small features [50]. Beside the imprint technology it is also possible to use the mold as an ‘ink’ stamp (Nano Imprint Lithography (NIL). The ink is a chemical solution with certain properties and is than applied to the substrate. Consequently it left the chemical on the contact area and after that it can be used as a mask.

2.2.5.1. Laser Assisted Direct Imprint (LADI)

This is an imprint technology that directly prints the mold in Si with the help of a laser beam. The mask is pressed into the molten layer. When the mask is removed, an accurate imprint of the component design remains in the silicon, with detail rendered at the 10-nm level. This technique proposed by [50] is called ‘Laser-assisted direct imprint’ (LADI). The process is given in Fig. 12. In this figure laser light passes through a quartz mask above the silicon surface (A & B). A single excimer laser pulse melts a thin surface layer of silicon, and a mould is embossed into the resulting liquid layer. The mask is pressed into the molten layer (Fig 12B) . When the mask is removed, an accurate imprint of the component design remains in the silicon, with detail

rendered at the 10-nm. The embossing time is less than 250 ns. In Fig. 12(D&E) a SEM image is given from a cross-section of the quartz mold (Fig.12D) and the Si imprint (Fig.12E). A uniform 300 nm period silicon grating is patterned and has a 140 nm line width and is 110 nm deep.

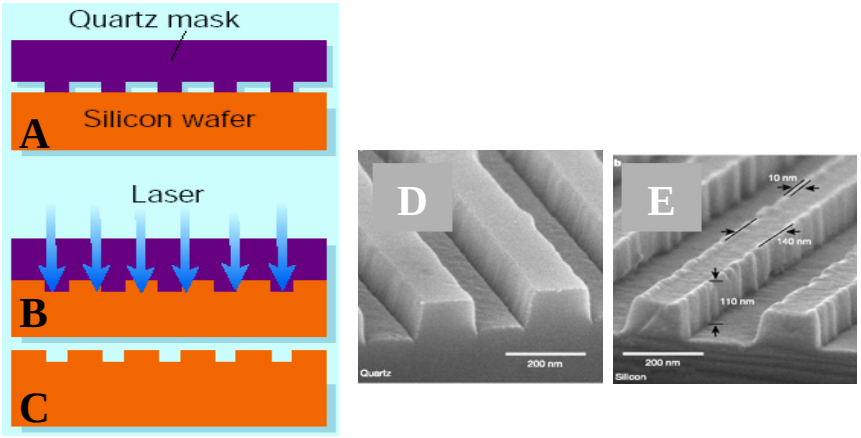

Figure 12. Laser-assisted direct imprint quartz mask is pressed into the molten Si layer heated by the laser light (A,B & C). SEM images of the quartz mold (D) and the imprinted patterns in silicon (E).

The mould after the two LADI processes showing no visible damage. The LADI area could be as large as a whole wafer (4 inch or 8 inch diameter). This method eliminates the costs because no expensive focusing optics and resist is needed.

2.2.6. Block copolymer template technology

Block copolymer consists of polymer chains made from two chemically distinct polymeric materials. Phase separation of the blocks leads to the formation of periodic nanoscale areas with a very uniform distribution of size and shape. Diblock copolymers spontaneously self organized themselves into micro domains. Such micro domain morphology can be used as a template for the formation of large area arrays of particles finally used as a template for nanostructures. Specials devices such as patterned media, waveguides require not only a long range ordering but also accurate pattern registration on a substrate without defects in their order. Various papers have been published to overcome the disorder such as directional solidification,

adding electric fields and topographic substrates creating by etching or chemical modification of the surface.

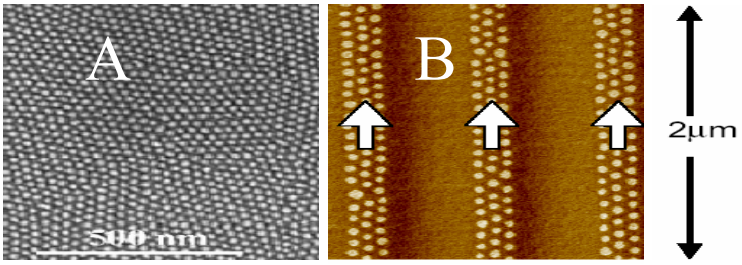

Figure 13. Self-assembled PS-PMMA island with 'domain boundaries' spinned on a smooth substrate (A) and in a grooved substrate the dots are aligned.

In Fig. 13A a self-organized block copolymer is spinned on a smooth substrate and defects (domain boundaries) are visible over short distances [51] while the block polymer is spinned over a grooved substrate (see Fig. 13B) the PMMA dots are now aligned along the groove direction. [51-53]. Another question is of course what the switching behavior is of large arrays of particles made by this method. Co particles have been made with 50-nm period arrays with 35 nm widths and 5-20 nm height [54]. The particles have in-plane anisotropy due to their shape.
In [55] a large-area fabrication of hexagonally ordered metal dot arrays with an area density of $\sim 10^{11}/cm^2$ was demonstrated. The metal dots were produced by an electron beam evaporation followed by a lift-off process. The dots size was 20 nm dots with a 40 nm period by combining block copolymer nanolithography and a trilayer resist technique. A self-assembled spherical-phase block copolymer top layer spontaneously generated the pattern, acting as a template. The pattern was first transferred to a silicon nitride middle layer by reactive ion etch, producing holes. The nitride layer was then used as a mask to further etch into a polyamide bottom layer.

2.2.7. Chemical ordering with ion irradiation

It is well known that chemical composition; crystal structure, grainsizes and their distribution are determining the magnetic behavior of thin films and dots. In thin films chemical ordered ferromagnetic phases such as FePt, FePd, and CoPt are very important for applications. This type of materials show the largest magnetic anisotropy in comparison with other

ferromagnetic films and that is due to the special chemical ordering in the L1O phase. To obtain chemical ordering high substrate temperatures are necessary (e.g. FePt 700K) [56]. High substrate temperatures are not suitable for production and consequently alternatives are generated such as the addition of third element, layer-by-layer growth, and also light ion irradiation. For instance He ions (20-150keV) can enhance the chemical ordering. Small energy transfers minimize recoil displacements to 1-2 interatomic distances. [57]. It has been observed [58] in co-sputtered FePt films that the long-range ordering parameter S (completely order (S=1) totally disorder material (S=0)) increases with the fluency (see Fig.15 (1)). In contrary ion irradiation can also be used to destroy the chemical ordering in alloys. A nice example is given in $CrPt_3$ thin films [59]. In the chemically ordered $CrPt_3$ with $L1_2$ phase (Cu_3Au) are the Cr atoms site at the corners and Pt atoms at the faces of a unit cell. This $CrPt_3$ phase is ferromagnetic, with the localized moments for Cr = 2.33mB and Pt = -0 27mB. The disordered phase is non magnetic and has a FCC structure and the Cr and Pt sites are randomly substituted. Consequently ion irradiation can locally transform chemically ordered CrPt3 into the chemically disordered FCC phase, which means that the ferromagnetic behavior is suppressed.

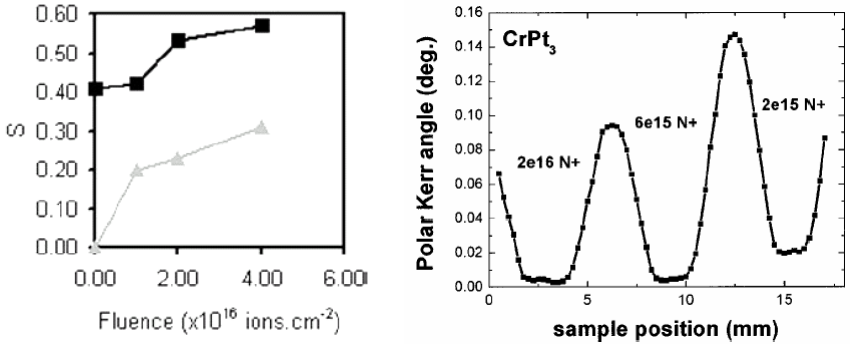

Figure 14. (left)Long-range order parameter S as a function of the fluency for a disorder FePt (50nm)-Pt (001) thin film (starting S=0) and particularly ordered one (starting S=0.4) and (right) Polar Kerr measurements of three irradiated $CoPt_3$ areas with N^+ ions with a fluency in the range $2x10^{15}$ - $2x10^{16}$ ions/cm^2.

Figure 14right shows the polar Kerr measurements of three irradiated $CoPt_3$ areas with N+ ions with a fluency in the range $2x10^{15}$ - $2x10^{16}$ ions/cm^2. The irradiated arias are 4x4 mm^2. The lowest dose is not sufficient to completely suppress the magnetic moment observed by the Kerr rotation while above 6x

10^{15} ions/cm^2 lead to a non-magnetic behavior. This opens the possibility for patterning magnetic and non-magnetic areas in a magnetic film.

3. MAGNETIC PROPERTIES OF PATTERNED THIN FILMS

It has been shown that size, shape, anisotropy and other properties determine strongly the magnetic behavior of a patterned thin film. Magnetization reversal processes of nanosized structures have been studied extensively from both of technical and scientific point of view. MOKE and MFM can observe reversal behavior of a collection of magnetic dots. A special high field MFM operating in vacuum and RT was used to analyze dots having perpendicular anisotropy. It is mounted in between the pole shoes of conventional electromagnet with a maximum field of 1353 kA/m (1.7T). The magnetic signal is detected at constant height, by means of phase measurement using a lock-in amplifier. A series of measurement was made with fields ranging from -1353 kA/m to 192 kA/m. We used here patterned CoNi/Pt multilayer films having a perpendicular anisotropy. [37,42].

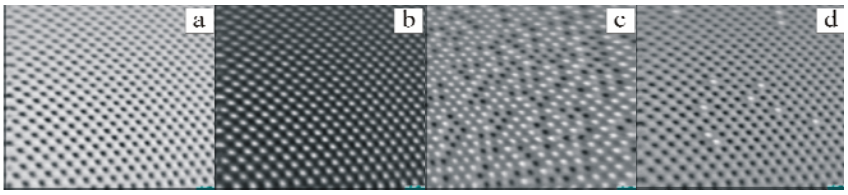

Figure 15. MFM images of a patterned CoNi/Pt multilayer after application of –1350, +4, +127 and +183 kA/m.

An example is shown in Fig.15. In this case for each image the field is increased to a certain value and taken back to zero, in order to minimize the influence of the tip on the sample. The first image of Fig. 15a shows the magnetization after applying -1353 kA/m perpendicular to the sample. The tip and medium are saturated in the same direction so only attractive forces occur (black dots). When field is increased to +4 kA/m, the tip reverses magnetization and all forces become repulsive, so the contrast reverses (white dots). At 127 kA/m almost 50% of the dots is reversed (Fig. 15c) and at 183 kA/m almost all the dots are reversed (Fig. 15d). The first dots switch already at 80 kA/m, but the last at 192 kA/m.

Studying the reversal mechanism of a single nano-dot is very difficult because the sensitivity of commercial magnetic analysis equipment is not

large enough. A few techniques aiming quantitative analysis need a complicated fabrication process and/or their working temperature is limited at low temperature. Analysis with Anomalous Hall Effect (AHE) for films with a perpendicular anisotropy have been proposed already for a long time [60,61] and it has been showed that this method belongs to the most sensitive measuring methods. The AHE gives information about the magnetic state of a ferromagnetic material, as it is proportional to the perpendicular component of the magnetization in the film or particle. Therefore data of relevant parameters such as Hc, Mr, S, Hk etc can be obtained by recording the hystheresis curves by plotting the AHE-voltage vs. the applied field. The sensitivity of the AHE measurements is very high in relation with SQUID and VSM –magnetometory (~ 10^{-15} emu).

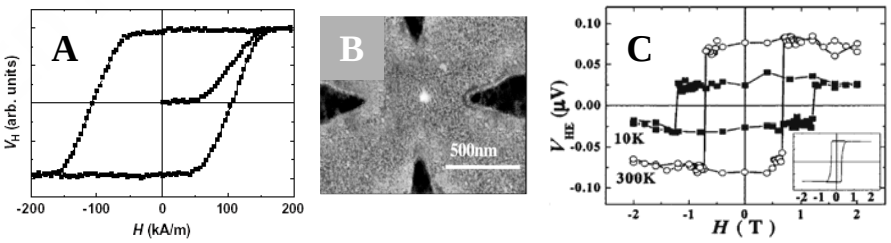

Figure 16. (A). The virgin curve and full AHE curve of a patterned Co/Pt multilayer with a dot size is 120nm. The loop is measured form about 200 dots in the area of the Hall cross, (B) SEM image of a 60 nm FePt dot (bright spot) covered with a Pt cross-shaped electrode, (C) AHE loops for 10 and 300 K with an inset of the un-patterned FePt film at 300 K.

In a recent paper the magnetization of an isolated dot prepared by e-beam lithography, from an L1o-FePt (001) film with a diameter of 60 nm has been measured by AHE, and moreover the analysis were carried out as function of temperature [62]. AHE measurement can be adapted to wide range of samples, from a single dot to an array of a few cm2 and as well as for very thin continuous films. Dot arrays made of polycrystalline Co/Pt multilayer with average grain size of 20 nm are fabricated [63]. Dot patterns of 200 nm thick positive resist for etching mask were exposed on the films by using Interference Lithography (IL) [37,42,63,64] and the patterns were transferred into the Co/Pt multilayers by using Ar+ ion beam etching (IBE). Arrays of circular dots of 120 nm and 200 nm in diameter were fabricated. In Fig.16(A) the virgin curve and full AHE hystheresis curve of a LI patterned Co/Pt multilayer [Pt (2 nm)/Co (0.5 nm)]5 / Pt (4 nm) consisting of 200 dots with a diameter of 120nm is presented. The energy barrier height of the dots

has been estimated as $4.0x10^{-12}$ erg, which corresponding to anisotropy energy of a column of 18 nm in diameter. The activation volume is comparable with the grain size measured with AFM. Recently [80] dot arrays of sub-micron diameter are fabricated from epitaxial grown $Co_{80}Pt_{20}$ film, which has large perpendicular anisotropy. Sweep rate dependent measurements has been carried out as well as angular dependent measurements.

The energy barrier height of reversal is estimated as 1.0×10^{-10}erg. The energy corresponds to the switching volume comparable with the volume of a physical grain in the dots. For a[application high anisotropy dots are very important. A promising material is the special $L1_O$ structure of FePt. In Fig.16(C) the result of AHE measurements on a single dot (60 nm in diameter) is given (see Fig 16(B)). Over the whole temperature range, the dot exhibit perfect rectangular magnetization loops with coercivity almost constant (Fig.16C). The activation energy has been evaluated to be about $4x10^{-19}$ J, equivalent to the domain-wall energy times the square of the domain-wall thickness, suggesting that the magnetization reversals are initiated by nucleation of reversed nucleus with the dimension of the exchange length.

Magnetic imaging and micromagnetic simulations have shown that non-uniform magnetization configurations in patterned structures can considerably affect the magnetization reversal [65].

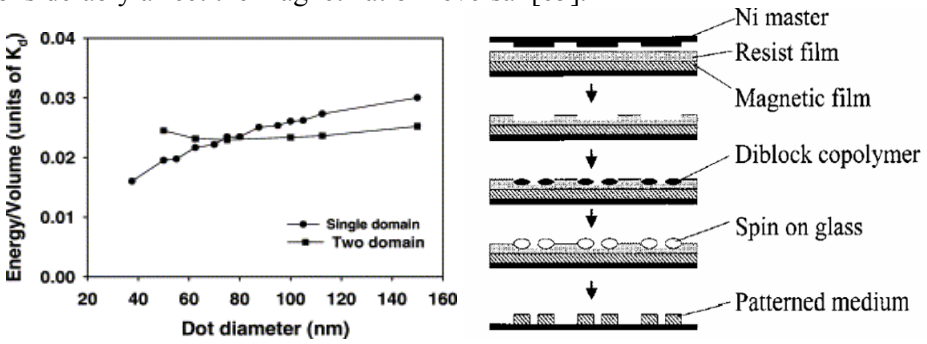

Figure 17. Micromagnetic simulations for a SD and MD state of CoNi/Pt dots with 30 nm thickness (left) and (right) the AASA process for a 2.5 inch disk.

In [66] results are presented from an investigation of the domain structure and magnetization reversal of small circular elements results by use of an existing micromagnetic simulation package. Such a study can contribute to

understand the behavior of patterned media for high-density recording and also, but also for non-volatile magnetic memories [67]. Later we use the micromagnetic simulation to study the critical size at which the energy of single domain state (SD) equals that of the two-domain state (TD or MD=multi-domain state) [68]. We also started to simulate the switching field distribution of such SD dots. By investigating stable configurations from different initial configurations and comparing the energies as a function of cell size, a set of equilibrium states are found. Using this procedure, the energy of dots of height 30 nm in SD and TD states are calculated as a function of dot diameter. Figure 17 (left) shows the calculated total minimum energy density as a function of dot diameter for the SD and MD states. Experimental results give more or less the same value for the critical size [37]. During the fabrication of nanostructures by using dry etching methods a very critical point is the damage of the ions made into the structures. Beside etch damage also imperfect layer growth might influence the switching field. Systematic influences of this kind of factors are discussed in [68]. An example is the slanting of the sidewalls of the dots, resulting from the imperfect resist pattern shape. Magnetization reversals of CoNi/Pt multilayer dots with (a) cylindrical, (b) pointed cone, and (c) truncated cone shape have been simulated and show all different hystheresis properties.

4. APPLICATIONS OF PATTERNED MAGNETIC FILMS

Patterned magnetic thin films are not only interested from the physics point of view but have also many different applications in the field of magnetism. Data storage, magnetic field sensing, logical elements and in bio-detection one can find different alternatives for applications. In this section we briefly discussed only the application of magnetic logic and high density magnetic.

4.1. Media for Ultrahigh-Density Magnetic Storage

The stability of written data becomes more and more a major concern in hard-disk design. The areal bit density of magnetic disk recording has increased enormously over the last decades. Extrapolation leads to bit densities not likely to be achieved without changes the way that the data is stored in the present media. Recently, laboratory demos have shown more than 160 Gbpsi. So far, scaling the critical physical dimensions of the hard disk was sufficient to double the density on an annual basis. Experimental

results and theory have shown that there is a limit to this scaling. Many alternative technologies have been proposed (see e.g. chapter 11) To overcome the problems of continuous media; patterned media is suggested as one of the potential ways for further increasing the areal recording density.

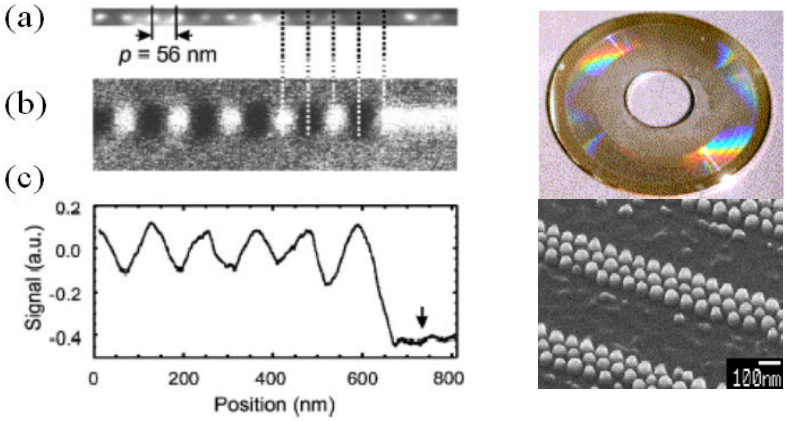

Figure 18. (left) GMR readback signals (c) from a single array of CoPtCr dots made by FIB. The AFM (a) image shows dots (period: 56nm and size:26nm) and MFM images (b) gives the magnetic bit image and (right) resist imprint on a disk with the aligned magnetic CoCrPt particles (at the bottom).

It becomes clear if one compare between bits in a continuous polycrystalline film (500-1000 crystals per bit) and a patterned medium (1bit = 1 dot) that the highest density is present in the patterned medium. Moreover, the super-paramagnetic bit density limit of this type of medium is much higher than that of present thin film media. Also, the constraints on the writing and reading process itself are strongly reduced. Due to the single-domain nature of every dot, the writing of such a bit is an all or-nothing event and the head does not have to be positioned exactly above the bit. In contrast to continuous medium, however, a write synchronization scheme has to be implemented. For the design of a prototype patterned medium for recording several requirements are given in [e.g. 3].

Besides, Co/Pt multilayers, perpendicular granular CoCrPt thin film (20 nm thick), suitable for a recording medium, has also been prepared by using FIB [95]. The patterns are directly made in the film by using 30 keV Ga+ at a beam current of 1pA.The pattern trenches are 6 nm deep and square arrays

of magnetic isolated islands have been prepared in the range 65–500 nm. Based on MFM measurements it was concluded [69] that below 130nm diameter only single domain behavior was obtained.
With a quasi-static write/read tester, recording experiments have been performed [70,71]. In Fig 18(a,b) AFM and MFM data are given from a recorded single row of square dots. The GMR readback signal is given in Fig. 18 (c). The obtained density was larger than 200 Gbpsi. In continuous thin film media bits can be placed at any area of the disk. In the case of patterned media the write pulse must be synchronized to the patterning [72]. For the right synchronization requirements, the switching field of distribution of the media and the head field gradients are important. Perpendicular single pole heads in combination with a soft underlayer are also suggested [73].
To increase the density of a rotated disk in [52], artificially assisted self-assembling method (AASA) is introduced. This method is a combination of nanoimprint technology and the use of a diblock copolymer. The result is shown in Fig. 18(right). Here it can be clearly seen that an aligned array of small CoCrPt particles (40nm in diameter) are aligned in the groove of a hard disk (2.5 inch). Figure 17(right) shows a schematic illustration of the preparation method. Ni master possessing spiral patterns with 60-250 nm width lands and 400 nm width grooves was pressed into a resist film on a magnetic layer. Than the diblock copolymer (PMMA-PS) was cast into the grooves and annealed. After removing selectively the PMMA by an oxygen plasma treatment the resulting holes were filled with spin on glass (SOG) . The SOG dots are used as a mask for dry etching the magnetic film (CoCrPt).

4.2. Nanoscale magnetic elements and logic devices

In [74,75] micron sized NiFe ring-shaped sensors have been fabricated by standard photolithography and proposed as a bio-detection device. Such as sensor can detect the radial component of the dipolar-fringing field from a single, partially magnetized micron sized NiFe sphere mounted on an AFM cantilever. When the sphere is above the center of the ring the AMR response to this fringing field is strongly peaked and is minimized when the sphere is moved beside the ring.
Ferromagnetic rings are also been fabricated by using electron-beam lithography with a lift-off process for pattern transfer [76]. These nanoscale

ferromagnetic rings do have a smallest outer diameter of 90 nm, inner diameter of 30 nm and thickness of 10 nm.
Generally in computing data is stored in one place and processing in another. Various groups are proposing magnetic logic elements in which data can be stored and data can be processed [77]. Their proposal is based on MRAM elements that has two independent input lines and than it could, in principle operate as any one of four different logic operations - AND, OR, NAND or NOR gates - and lead to increased computational efficiency.

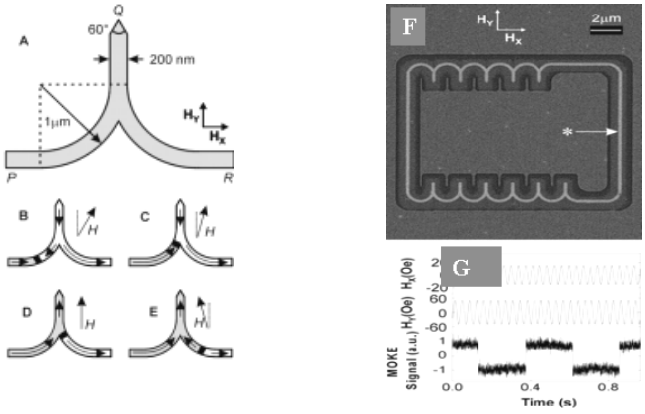

Figure 21. Schematics of the hairpin NOT gate (A) and the mechanism of the domain wall injection (B to E). In (F) the 11 NOT junctions are shown and in G the comparison of the MOKE analysis and the applied field components Hx and Hy.

Such type of device has many advantages over transistor-based logic and that it could lead to programmable magneto-logic circuits in the near future. Such system of interacting magnetic nano-cells can be produced today in the order of 100nm and as expected in the future in much smaller size (at least a factor 10 smaller) for the individual building blocks. Moreover such a system has a high speed (switching in magnetic films can be in the GHz) and non-volatility and can operate at room temperature.
A so-called quantum-dot cellular automata (QCA) was proposed by [78], which employs arrays of coupled quantum dots to implement Boolean logic functions [79] The advantage of QCA lies in the extremely high packing densities possible due to the small size of the dots, the simplified interconnection, and the extremely low power-delay product. Using QCA cells with dots of 20 nm, an entire full adder can be placed within 1 mm^2

[80]. A processing method based on magnetism is also given in [81]. Here networks of sub-micrometer magnetic dots are used to perform logic operations and propagate information. The logic states are signaled by the magnetization direction of the single-domain dots and the dots are coupled to there nearest neighbors through magnetostatic interaction. In [81] QCA-network is shown and consist of single elongated input dot followed by a chain of 69 circular dots (110nm in diameter) [81]. The dots are 10 nm thick and made from Supermalloy and fabricated with e-beam lithography.

Magnetic solitons carry information through the networks, and an applied oscillating magnetic field feeds energy into the system and serves as a clock. These networks offer a several thousand-fold increase in integration density and a hundredfold reduction in power dissipation over current microelectronic technology. The fact that the entire network can be fabricated on a single plane means that many planes could in principle be stacked on top of each other, thus giving a way to realize 3D hardware. In addition also the building blocks for a logic systems such as a NOT gate are studied [82,83]. An all-metallic sub micrometer device is demonstrated experimentally at room temperature that performs logical NOT operations on magnetic logic signals. When this two-terminal ferromagnetic structure is incorporated into a magnetic feedback loop, the junction performs a frequency division operation on an applied oscillating magnetic field. Up to 11 of these junctions are then directly linked together to create a magnetic shift register. The device is fabricated with a FIB from 5 nm thick Permalloy and a full description of the device is given in [82].

In Fig.21(A) first of all the metallic ferromagnetic NOT gate is shown with line width of 200nm and a hairpin shape. The operation concept of the NOT gate magnetization reversal is shown in fig B to E with the magnetization directions (arrows) in the various parts of the hairpin and the domain wall (thick line) motion as a consequence of rotating applied magnetic field by components Hx and Hy. In Fig.21F the FIB image of a magnetic ring including 11 NOT junctions, is given with the asterisk indicating the position of subsequent MOKE analysis which is given in (G) The MOKE analysis gives an identical structure with the clockwise-rotating magnetic field components.

Domain wall control is an intensive subject of study because it can lead to new logic and memory devices. Domain walls can be injected into planar magnetic nanowires either from magnetically soft large-area “pads” or by using the local magnetic field from an overlying current-carrying wire. The domain wall resistance, magneto resistance, domain wall displacement are

measured A complete nano-magnetic logic system can only work if it is interfaced with conventional electronics. Data can be written in magnetite structures by a current-carrying strip line and data can be read out by incorporating spin tunnel junctions or spin valves into magnetic tracks or alternatively by measuring domain wall resistance.
For non-volatile memory devices it would be a great advantage if a magnetic bit could be switches by the current passing through it, rather than by some external magnetic field. If so the design of high-density non-volatile memory would be greatly simplified. In [84] spin-polarized current switching of a Co thin film nanomagnets (60 nm x 130nm) is discussed.

5. CONCLUSIONS

Patterned magnetic nanostructures are researched and developed for fundamental studies and applications. It is clear that there is a growing interest in making well-defined structures of magnetic thin films with nanodimensions. Especially the fields of magnetic recording, sensors, logic systems, MRAM and spin-electronics have shown great interest in nanosized structures. There is a tradeoff form the area of patterning and the accuracy, the size of the individual dots or wires and the price of the equipment and the related technologies. With some of the techniques it is possible to realize structures smaller than 10 nm over a relatively large area. For future applications the price will be a dominant factor.
The properties are always influenced by the structural properties of the continuous film and moreover also the fabrication technologies can have a large influence on the nanosized structure. Important hereby are the application of the dry etching (implantation, roughening of the sidewalls etc.) and redeposition at the side walls due to the etching.
It has been showed that the size and shape of nanostructures plays an essential role in determining the magnetic properties. One critical size of a structure is the SD or MD state. In certain materials the magnetic anisotropy can be influenced by size, shape and configurational anisotropy and in others the crystalline perfection determines the anisotropy.
The analysis of magnetic nanoelement is not simple due to their small volume. We need sensitive methods. MFM, MOKE and SQUID measurements can give us help in understanding the magnetic behavior of such a small elements. Micromagnetic simulations are of great help to understand the behavior and to help with designing the structure. For understanding the individual particle we need to develop new analysis

method. In our application particles with perpendicular anisotropy can be analyzed by the AHE and it has been shown that this method is very sensitive because the hystheresis loop of a single FePt of 60 nm has been measured. For application is also important that we use array of particles. In that case we have to deal with the interaction between the dots due to the dipolar fields. This is very important for application because these effects will influence the Hc and switching field distribution of the array It has been shown that small patterns can principally be made in circular patterns, which is interesting for hard disk application. Alternatively by using the AASA-method have shown the circumferential magnetic patterned hard disk media with 40 nm diameter on a 2,5 inch disk. This method uses the nanoimprint technique of making land-groove spirals using self-assembling diblockpolymer aligned in the groove. The most fascinating area of study and application can be find in the area where different disciplines are meeting each other such as magnetism with, biology, superconductivity, molecules, semiconductors etc.

From the technology point of we are able to realize a variety of structure and dimensions using different kind of materials. But the technology effects in relation with scaling down the dimensions means that we are far of the complete understanding of the properties of the nanosized structures. One of the most important tasks is to understand the magnetization reversal of nanosized dots and the interaction between dots. Dynamic measurements of the magnetic properties are extremely important for application. A good example is here the application in the field of high data rates in relation with logic and computing. The requirement of patterning large areas of regularly spaced uniform dots at nano-dimensions puts strong demands on the patterning technology. Even in the R&D laboratories such technologies are generally not readily available, not to speak of technology for the manufacturing of a patterned hard disk, which is one of the possible application.

ACKNOWLEDGEMENT

The author thanks the SMI-group members for their contributions but like to mention specially the cooperation in this field with Leon Abelmann, N. Kikuchi, Nguyen Dao, Martin Siekman and Rogelio Murillo. The Dutch Technology Foundation (STW) financially supports this work.

REFERENCES

[1] J. P. Wang and T. J. Zhou in Encyclopedia of Nanoscience and Nanotechnolgy, Ed. by H.S.Nalwa Vol.8, 415, American Scientific Publishers, (2004).
[2] J.I. Martin, J. Nogues, Kai Liu, J.L. Vicent and Ivan K. Schuller J. Mag. Mag. Mat. 256, 449, (2003)
[3] J. C. Lodder, J. of Magn. and Magn. Materials, 272-276, 1692, (2004),
[4] R.P.Cowburn, J.Phys D: Appl.Phys. 33, R1 (2000)
[5] R.P.Cowburn, J.Magn.Magn.Mater. 242-245,505,(2002
[6].A.Dietzel,R.Berger,H.Grimm,W.H.Bruenger,C.Dzionk, F.Letzkus, R.Springer, H.Loeschner, E.Platzgummer, G.Stengl, Z.Z.Bandic and B.D.Terris, IEEE Trans. Magn. 38, 1952, (2002).
[7] S.Y.Chou, P.R.Krauss, P.J.Renstrom, Science, 272, 85-7, (1996)
[8] (S.Y.Chou, P.R.Krauss, W.Zhang, L.Guo and L. Zuang, J.Vac.Sci.Technol.B 15(6), 2897 (1997)
[9] C.Chappert, H. Bernas, J. Ferre, V. Kottler, J.-P. Jamet, Y. Chen, E. Cambril, T. Devolder, F. Rousseaux, V. Mathet, and H. Launois, Science 280, 1919 (1998).
[10] T Devolder, J. Ferre, C. Chappert, H. Bernas, J.-P. Jamet, V. Mathet, Phys. Rev. B 64, 064415 (2001).
[11] E. E. Baglin, M. H. Tabacniks, R. Fontana, A. J. Kellock, and T. T. Bardin, Mater. Sci. Forum, 248-249, 87 (1997).
[12] T. Devolder, Phys. Rev. B 62, 5794, (2000).
[13] A. Mougin, T. Mewes, M. Jung, D. Engel, A. Ehresmann, H. Schmoranzer, J. Fassbender, B. Hillebrands, Phys. Rev. B 63, 060409 (2001).
[14] A.Traverse, M.G.Boite, G.Martin, Europhys.Lett.8 (7), 633, (1989)
[15] T. Devolder, C. Chappert, Y. Chen, E. Cambril, H. Bernas, J. P. Jamet, and J. Ferre, Appl. Phys. Lett. 74, 3383 (1999).
[16] B. D. Terris, D. Weller, L. Folks, J. E. E. Baglin, and A. J. Kellock, J. Appl. Phys. 87, 7004, (2000)
[17] T.Aign,P. Meyer, S. Lemerle, J. P. Jamet, J. Ferré, V. Mathet, C. Chappert, J. Gierak, C. Vieu, Phys.Rev.Lett.81 (25) 5656 (1998).
[18] C.T.Rettner, M.A. Best, B.D.Terris, IEEE Trans.Magn.37(4), 1649, (2001).
[19] R.Allenspach, A. Bischof, U.Durig, P Grutter.,Appl.Phys.Lett.73(24), 3598, (1998)
[20] T.J.Zhou, Y.Zhao, J.P.Wang, T.C.Chong, J.Y.L.Thong, IEEE.Magn.,38(5), 1970, (2002)
[21]M.Zheng, M.Yu,Y.Liu, R.Skomski, S.H.Liou, D.J.Sellmyer, V.N.Petryakov, Yu.K.Verevkin, N.I.Polushkin,and N.N. Salashchenko, Appl.Phys.Lett.79,2606 (2001)
[22] M.Yu, Y.Liu, D.J.Selmyer, J.Appl.Phys., 85, 4319,(1999).
[23] G.Thornell, S.Johansson, J. Micromech. Microeng. 8, 251 (1998)
[24]. A.Lipicki, K.Kang, T.Suzuki, IEEE Trans.Magn.,38(5), 32589,(2002)
[25] S.I.Woods, S.Ingvarsson, J.R.Kirtley, H.F.Hamann, R.H.Koch, APL, 81(7), 1267 (2002)
[26] E.O.Samwel, D.B.Bijl, J.C.Lodder,Th.J.A.Popma, J.Magn.Magn.Mat., 155, 292 (1996).
[27] J. Ferre, C. Chappert, H. Bernas, J.-P. Jamet, P. Meyer, O. Kaitasov, S. Lemerle, V. Mathet, F. Rousseaux, H. Launois J.Magn.Magn.Mater.198-199, 191, (1999)
[28] D. Weller, J. E. E. Baglin, A. J. Kellock, K. A. Hannibal, M. F. Toney, G. Kusinski, S. Lang, L. Folks, M. E. Best, and B. D. Terris, J.Appl.Phys.87(9), 5768, (2000)
[29] C.T.Rettner, S.Anders, J.E.E.Baglin,T.Thomson, B.D.Terris, Appl.Phys.Lett.80(2), 279, (2002).

[30] S. P. Li, W. S. Lew, J. A. C. Bland, L. Lopez-Diaz, M. Natali, C. A. F. Vaz , Y. Chen, Nature,Vol 415, 600, (2002).
[31] H.Loescher, E.J. Fantner, R.Kornter, E. Platzgummer, G.Stengl, M.Zeininger, J.E.E.Baglin, R.Berger, W.H. Bruenger, A Dietzel, M.I. Baraton, L. Merhari, Proc. MRS Vol. 739, 3, (2003).
[32] L.F.Johnson, G. W. Kammlott, K. A. Ingersoll, Appl.Opt.17, 1165, (1978)
[33] Wei Wu,Bo Cui, Xiao-yun Sun, Wei Zhang, Lei Zhuang, Linshu Kong, Stephen Y. Chou, J.Vac.Sci.Technol.B 16, 3825, (1998)
[34] M.L. Schattenburg, C.R. Canizares, D. Dewey, K.A. Flanagan, A. Hammett, A.M. Levine, K.S.K. Lam, R. Manikkalingam, T. Markert, and H.I. Smith, Opt.Eng.30,1590, (1991)
[35] E.F.Wassermann, M. Thielen, S. Kirsch, A. Pollmann, H. Weinforth, A. Carl, J.Appl.Phys.83,1753, (1998)
[36] M.Farhoud, M. Hwang, H.I. Smith, M.L. Schattenburg, J.M. Bae, K. Youcef-Toumi, C.A Ross,. IEEE Trans.Magn.34, 1087, (1998)
[37] M.A.M.Haast, J.R. Schuurhuis, L. Abelmann, J.C. Lodder, Th.J., IEEE Trans.Magn.34, 1006, (1998)
[38] J. P. Spallas, R. D. Boyd, J. A. Britten, A. Fernandez, A. M. Hawryluk, M. D. Perry,
D. R. Kania, J.Vac.Sci.Technol.B 14, 2005, (1996)
[39) T. A. Savas, M. L. Schattenburg, J. M. Carter, H. I. Smith, J.Vac.Technol.B 14, 4167,(1996)
[40] W.Hinsberg, F. A. Houle, J. Hoffnagle, M. Sanchez, G. Wallraff, M. Morrison, S. Frank., J.Vac.Sci.Technol.B 16, 3689, (1998)
[41] T.A. Savas, S.N. Shah, M.L. Schattenburg, J.M. Carter, H.I. Smith, J. Vac. Sci. Technol , B 13, 2732, (1995)
[42] R.Murillo, H.A.van Wolferen, L.Abelmann, J.C.Lodder, in press Micr. Eng. (2005).
[43] J. Moritz, L. Buda, B. Dieny, J. P. Nozie`res, R. J. M. van de Veerdonk, T. M. Crawford, and D. Weller, Apll.Phys.Lett.,84(1), 1519, (2004)
[44] S. Matsui,Y. Igaku, and H. Ishigak, J. Fujita, M. Ishida, and Y. Ochiai, M. Komuro, H. Hiroshima, J.Vac.Sci.Techn., B12, 2801,(2001)
[45] Babak Heidari, Ivan Maximov, Lars Montelius, J.Vac.Sci.Technol.B 18(6), 3557, (2000)
[46] Jan Haisma, Martin Verheijen,a) Kees van den Heuvel, Jan van den Berg
J.Vac.Sci.Technol.B 14(6), 4124,(1996)
[47] T.Bailey,et al.,. T. Bailey, B. J. Choi, M. Colburn, M. Meissl, S. Shaya, J. G. Ekerdt, S. V. Sreenivasan, C. G. Willson, J.Vac.Sci.Technol.B 18, 63572, (1996)
[48] Gary M. McClelland, Mark W. Hart, Charles T. Rettner, Margaret E. Best,
Kenneth R. Carter, and Bruce D. Terris, Appl.Phys.Lett.81 (8), 1483, (2002)
[49] F.Carcenac, C. Vieu, A.Lebib, Y.Chen, L. Manin-Ferlazzo, H.Launois,
Microelct.Eng.53, 163,(2000).
[50] L.Jay Guo, J.Phys.D: Appl.Phys. 37, R132 (2004)
[51] J.Y.Cheng, C.A.Ross, E.L.Thomas, H.I.Smith, G.J.Vancso, Adv.Mater, 15, 1599, (2003)
[52] K.Naito,H.Hieda,M.Sakurai,Y.Kamata,K,Asakawa,IEEE.Trans.Magn,38(5),1949, (2002)
[53] A.Kikutsi, Y.Kamata, H.Hieda, M.Sakurai, K,Asakawa, K.Naito, Trans. Magn. Soc. Japan, 4, 1, (2004)
[54] J. Y. Cheng, C.A.Ross, E.L.Thomas, H.I.Smith, R.G.H.Lammertink, G.J.Vancso IEEE Trans.Magn.38 (5), 2541, (2002)
[55] M.Park, P.M.Chain,R.A.Register,D.H.Adamson, APL, 79(2),257, (2001)

[56] R. F. C. Farrow, D. Weller, R. F. Marks, and M. F. Toney. S. Hom, G. R. Harp, A. Cebollada, Appl.Phys.Lett.,69,1166, (1996)
[57] J.Fassbender, D.Ravelosona, Y.Samson, J.Phys.D: Appl.Phys. 37, R179, (2004)
[58] D. Ravelosona, C Chapper,V. Mathet, H. Bernas, Appl. Phys. Lett. 76 236(2002).
[59] Olav Hellwig, Dieter Weller, A. J. Kellock, J. E. E. Baglin, Eric E. Fullerton, Appl.Phys.Lett 79(8),1151, (2001)
[60] S. de Haan, J. C. Lodder , J Magn Magn Mater, 155(1-3) , 193, (1996),
[61] B.C.Webb, S.Schulz, S.B.Oseroff, J.Appl.Phys.,63(8),2923, (1988).
[62] N. Kikuchi, S. Okamoto, O. Kitakami, Y. Shimada, and K. Fuakmichi, Appl. Phys. Lett. 82 4313,(2003)
[63] N. Kikuchi, R. Murillo, and J. C. Lodder, accepted for publication JMMM 2005.]
[64] N.Kikuchi, R.Murillo, J.C.Lodder, K.Mitsuzuka, T.Shimatsu, Digest….. Intermag, Nagoya, March, 2005.
[65] Shi, T. Zhu, M. Durlam, E. Chen, S. Tehrani, Y.F. Zheng and J.-G. Zhu IEEE Trans. Magn. 34, 997, (1998)
[66] K. Ramstock, J.J.M. Ruigrok, J.C. Lodder, Sensors & Actuators A 81(1–3), 359, (2000)
[67] G.A. Prinz, Science 282,1660, (1998).
[68]. S. Sindhu, M.A.M. Haast, K. Ramstock, L. Abelmann, J.C. Lodder,
J. Magn.Magn.Mater., 238,246, (2002)
[69] C.T. Rettner, M.E. Best, B.D. Terris, IEEE Trans. Magn. 37(4) 1649, (2001)
[70] J. Lohau, A. Moser, C. T. Rettner, M. E. Best, B. D. Terris, Appl.Phys.Lett.78 (7) 990. 2001)
[71] M.Albrecht, C. T. Rettner, A. Moser, M. E. Best, B. D. Terris, Appl.Phys. Lett.80 (18),3409, (2002).
[72] M.Albrecht C. T. Rettner, A. Moser, M. E. Best, and B. D. Terris Appl.Phys. Lett.81 (15), 2875, (2002).
[73] G.F. Hughes, IEEE Trans. Magn. 36 (2), 521, (2000).
[74] G. A. Prinz, J. Magn. Magn. Mater. 200, 57 (1999).
[75] M. M. Miller, G. A. Prinz, S. -F. Cheng, S. Bounnak, Appl. Phys. Lett. 81, 2211 (2002).
[76] L.J..Heyderman, C.David, M.Klauui, C.A.F.Vaz, J,A.C.Bland, J. Appl. Phys., 93(12), 10011, (2003)
[77] A.Ney, C.Pampuch, R.Koch, K.H.Ploog, Nature, 425, 485, (2003)].
[78] C. S. Lent, P. D. Tougaw, W. Porod, and G. H. Bernstein, Nanotechnology 4, 49 (1993)
[79].P. D. Tougaw and C. S. Lent, J. Appl. Phys. 75, 1818 (1994)
[80] G.L.Snider, A.O.Orlov, I.Amelani, X.Zuo, G.H.Bernstein, C.S.Lent, J.L.Mertz, W.Porod, J.Appl. Phys., 85(8),4283 (1999)
[81] R.P.Cowburn, M.E.Welland, Science 287, 1466 (2000)
[82] D. A. Allwood, G. Xiong, M. D. Cooke, C. C. Faulkner, D. Atkinson, N. Vernier and R. P. Cowburn. , Science, 296, 2003, (2002)].
[83] D. A. Allwood, Gang Xiong, and R. P. Cowburn , Appl. Phys. Lett. 85, p.2848 (2004).
[84] F. J. Albert, J. A. Katine, R. A. Buhrman, and D. C. Ralph, Appl. Phys. Lett. 77, 3809, (2000)